

3D ELECTRIC FIELD COMPUTATION OF OPTIMISED HIGH-VOLTAGE INSULATOR USING PSO-FEM COUPLED ALGORITHM

Dyhia Doufene,* Slimane Bouazabia,* and Sid A. Bessedik**

Abstract

The purpose of this study is to estimate 3D electric field distribution on a polluted suspension insulator surface using finite element method (FEM) combined with a metaheuristic method namely a particle swarm optimization (PSO) algorithm. The PSO is applied to reshape an insulator form that presents a better electrical performance and thus reduce the electric field at the pin region. In the presence of pollution, this region is proved to be the most critical area for discharge initiation and propagation. The study of the electric field repartition on optimized high-voltage (HV) insulators under polluted conditions plays an important role in enhancing the performance and reliability of HV insulators. For this purpose, the electric field is calculated in both dry clean and contaminated surface conditions using FEM. Afterwards, the PSO algorithm is proposed as an efficient approach for optimizing the insulator geometry. Each stage of the work will be studied in both clean and polluted situations. From the achieved results, we see that the hybrid algorithm (PSO-FEM) gives great aptitudes for enhancing the distribution of the electric field on the HV insulators. The proposed PSO-FEM algorithm could be very helpful tool for designing HV insulator profiles that provide enhanced performances.

Key Words

Insulators design, particle swarm optimization, finite element method, 3D electric field

1. Introduction

The use of optimization techniques to improve the electrical performance of high-voltage (HV) insulators has increased significantly in the recent years [1]–[11]. Due to their simplicity, derivation-free mechanism, and local optima avoidance [12], meta-heuristic optimization techniques are increasingly adopted for engineering design problems. Among the most popular meta-heuristics, the

particle swarm optimization (PSO) algorithm is chosen for this study. This work is focused on the optimization of HV insulators in the presence of pollution, which is the most important contribution made in this work given the absence of work in this axis of study. Indeed, all works done are carried out in the clean case [1]–[10]. The only work done in the presence of pollution by Doufene *et al.* [11] with a coupled artificial neural network (ANN)-genetic algorithms (GA) and In [11] using a coupled ANN-(PSO) uses a predicted function of the electric field by mean of the ANN.

The advantage of the present work is the use of the real value of the electric field as a fitness function, thanks to finite element method (FEM) code developed in the “electric current” interface of COMSOL Multiphysics using the live link to MATLAB that gives a possible coupling with the PSO code. As reported in the literature, the high electric field value is the most important factor in the initiation and evolution of the discharge on the surface of a polluted insulator [2], [3].

All works carried out regarding the electric field calculation on the leakage path of high-voltage insulators agreed that the maximum value is always located at the pin region [14]–[20]. So to better prevent the flashover of suspension insulators, a knowledge of the distribution of the electric field at its outer surface is essential. In this optimization problem, the electric field value at the pin region is taken as a fitness function to be optimized (minimized). The different lengths of the insulator ribs are taken as the optimization variables. The work is divided into two parts: first, the FEM is used by mean of COMSOL Multiphysics to compute the fitness function (the electric field at the pin region), and second, the COMSOL Mutliphysics model is converted to a MATLAB code, *via* the live link to MATLAB, that will be coupled with the PSO code to perform the optimization (minimization of the electric field). This work is done in both clean and polluted cases.

2. Methodology of the Research

In this paper, 2D and 3D electric field and potential repartitions along suspension insulator surface were calculated by using FEM software COMSOL Multiphysics. PSO has

* Electrical engineering Department, University of Science and Technology Houari Boumediene (USTHB), 16123 Algeria; e-mail: {doufenedyhia, sbouazabia}@yahoo.fr

** Université Amar Telidji Laghouat, Laghouat, 03000 Algeria; e-mail: s.bessedik@lagh-univ.dz

Corresponding author: Dyhia Doufene

Recommended by Dr. Shuhui Li
(DOI: 10.2316/J.2023.203-0428)

Table 1
Parameters of the Insulator

Dimensions [cm]			Applied Voltage [V]	
Shed diameter (D)	Unit spacing (H)	Creepage distance (L)	pin	Cap
32.0	20.5	55	10,000	0

Table 2
Electrical Conductivity and Permittivity of the Used Materials

Materials	Permittivity	Conductivity [S/m]
Air	1	0
Glass	5.59	10^{-14}
Iron	106	$5,99.10^7$
Cement	5.9	10^{-12}
Pollution	80	10^{-4}

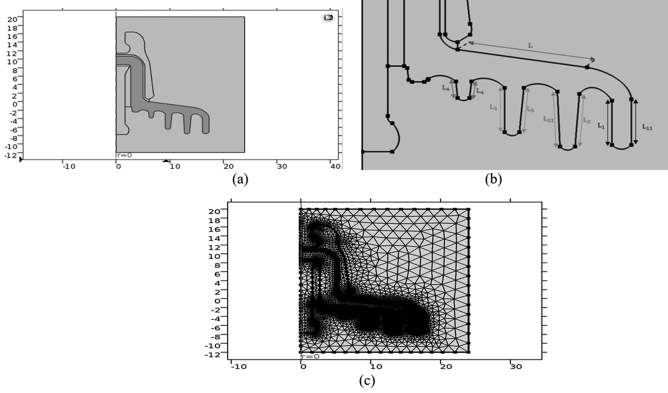


Figure 1. (a) Insulator profile; (b) optimization variables; and (c) mesh surface.

been proposed as an optimization method to design an optimal insulator profile. Then, the coupled approach based on PSO-FEM is employed to optimize the electric field value on the upper surface of this HV suspension insulator.

This section discusses the proposed methodology which comprises potential and electric field calculation in both 2D and 3D configurations, case studies before optimization, optimization process using PSO, and case studies after optimization.

2.1 Potential and Electric Field Calculation

The U400B suspension insulator taken from practical insulators used in the Algerian electrical grid is adopted in this study [21]. The insulator parameters are summarized in Table 1. COMSOL Multiphysics software is used to reproduce the insulator geometry, as shown in Fig. 1(a). In the parameter section of the geometry construction, the lengths (L1 to L4), given in Fig. 1(b), are considered as the optimization variables. Table 2 gives the electrical parameters of the model. The mesh is shown in Fig. 1(c).

(1) and (2) are solved using FEM [22] to calculate potential and electric field distributions:

$$\Delta V = 0 \quad (1)$$

$$\vec{E} = -\vec{\nabla}V \quad (2)$$

where \vec{E} represents the electric field and V is the electric potential.

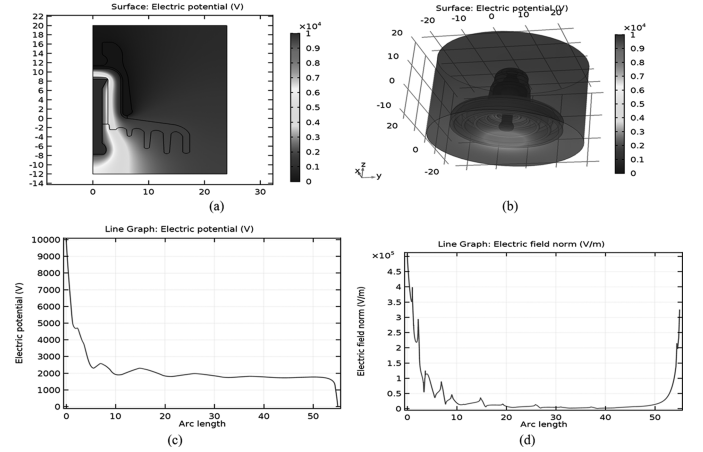


Figure 2. Clean case results. (a) 2D electric potential surface distribution; (b) 3D electric potential surface distribution; (c) potential distribution on the leakage path; and (d) electric field distribution on the leakage path.

2.2 Cases Studies before Optimization

2.2.1 Clean Case

Figure 2(a) and (b) give the surface distribution of the electric potential on 2D and 3D representations, respectively. Figure 2(c) giving the potential distribution on the leakage path of the insulator shows a variation between 0 kV in the cap and a maximum of 10 kV in the pin region.

In all the figures, the potential and the electric field distributions are represented from the pin to the cap region. The electric field distribution as shown in Fig. 2(d) confirms that there are two regions where its values reaches a maximum: around the cap with a value of 3.25 kV/cm and around the pin where it reaches its maximum value of 5,08 kV/cm.

2.2.2 Polluted Case

To analyse the behaviour of the insulator in the polluted case, a pollution layer of 0.5 mm (Fig. 3) is deposited on the upper surface of the insulator. The electrical conductivities of the different materials are given in Table 2.

Figure 4(a) shows a distribution of electric potential after the pollution deposition, and Fig. 4(b) gives the

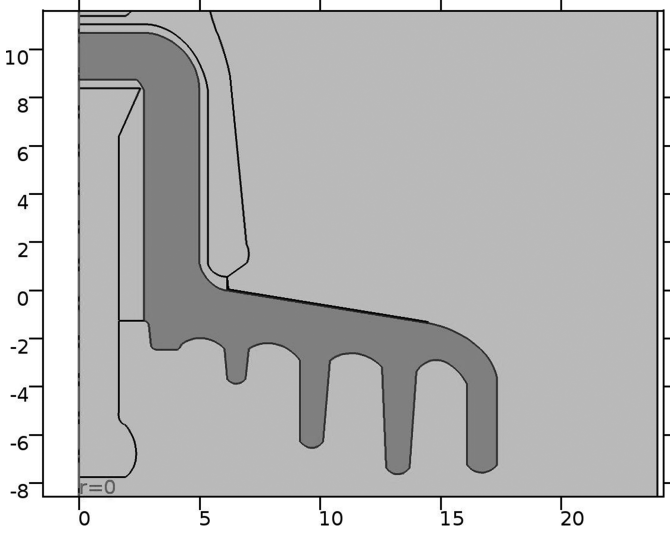


Figure 3. Zoom in the pollution layer.

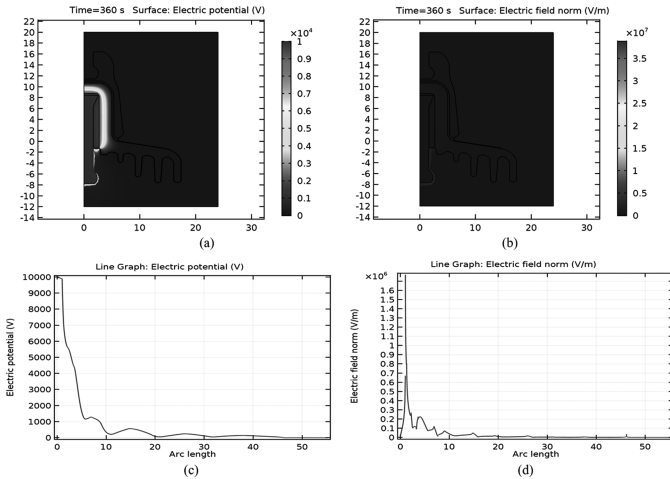


Figure 4. Polluted case results. (a) 2D electric potential surface distribution; (b) electric field surface distribution; (c) potential distribution on the leakage path; and (d) electric field distribution on the leakage path.

surface distribution of the electric field. The change in the potential distribution on the leakage path of the insulator after the pollution deposition is illustrated in Fig. 4(c). The electric field value rises to 17.7 kV/cm at the pin region as shown in Fig. 4(d) and decreases to 0 kV/cm in the cap region.

2.3 Optimization Process using PSO

The PSO is an efficient global optimization algorithm for such optimization problems. Presented by Kennedy and Eberhart [23, 24], the PSO is inspired from the relationships of travelling birds and the way they optimize their movements when travelling long distances searching for food.

The PSO algorithm is summarized as follows:

- Random positions and velocities are given to an initial swarm. The optimization variables l_1 , l_2 , l_3 , and l_4

are represented by the vector of positions $(x_i)^T(t)$ (3). The population of the swarm is defined by a matrix $P(i, j)$ (4):

i from 1 to n ; n = population size.

j from 1 to 4; 4 = optimization variables.

$$x_i(t) = [l_1 \ l_2 \ l_3 \ l_4] \quad (3)$$

$$P(i, j) = \begin{bmatrix} l_{11} & l_{12} & l_{13} & l_{14} \\ l_{i1} & l_{i2} & l_{i3} & l_{i4} \\ l_{n1} & l_{n2} & l_{n3} & l_{n4} \end{bmatrix} \quad (4)$$

- The fitness function (electric field) is computed for each particle of the matrix $P(i, j)$. The particle with the minimal fitness in the swarm is set as the best position ($P_i(t)$).
- The global solution ($g(t)$) that represents the particle having the minimal fitness function in the swarm is selected.
- The velocity, the position, and the inertia weight of each particle (5) are updated:

$$\begin{cases} v_i(t+1) = w(t)v_i(t) + C_1r_1(t)(P_i(t) - x_i(t)) \\ \quad + C_2r_2(t)(g(t) - x_i(t)) \\ x_i(t+1) = x_i(t) + v_i(t+1) \\ w(t) = w_{\max} - \frac{w_{\max} - w_{\min}}{t_{\max}} t \end{cases} \quad (5)$$

where $w(t)$ is the inertial weight, $r_1(t)$ and $r_2(t)$ are random values (in the interval [0 1]), C_1 and C_2 are acceleration constants (regulating the velocities), w_{\max} is the initial weight, w_{\min} is the final weight, and t is the number of iterations.

- The process is repeated, from step 2, until the stopping criteria is satisfied. The stopping criterion is set to 150 iterations.
- The best particle solution is displayed. The verification on COMSOL Multiphysics is done.

In this study, the fitness function associated with the maximum value of the electric field can be defined in [9, 12].

2.4 Cases Studies after Optimizations

The PSO parameters selected for this study are maximum number of iterations $\text{Maxiter} = 150$ and learning factors $C_1 = 1$ and $C_2 = 3$. As demonstrated in [9], 10 individuals are enough to solve this optimization problem.

2.4.1 Clean Case

After the optimization process, the convergence curve of the electric field along the iterations is given in Fig. 5(a). Figure 5(b) gives the variation of the optimization variables. The shape of the optimized model is shown in Fig. 6. The detailed values of the optimized model are summarized in Table 3. The electric potential distribution

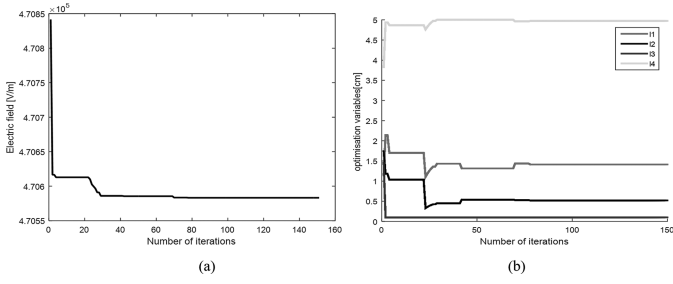


Figure 5. Optimization results in the clean case. (a) The convergence curve and (b) the variation of the optimization variables.

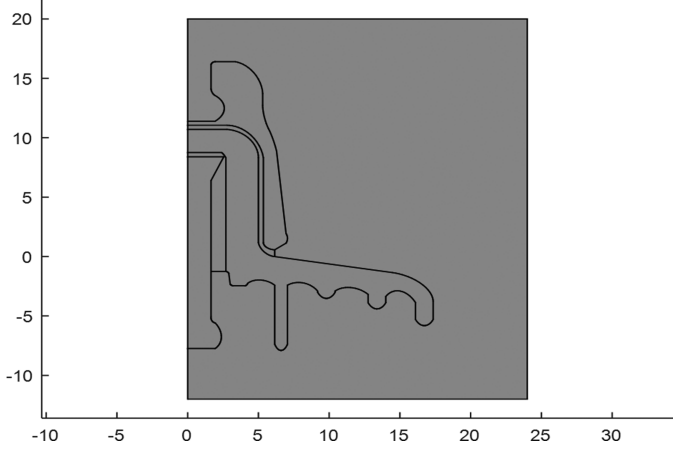


Figure 6. The shape of the obtained insulator after optimization (clean case).

Table 3
Details of the Optimized Values in Clean Case

	Reference Model	Optimized Model
l_1 [cm]	3,30	1.41
l_{11} [cm]	3,40	1,51
l_2 [cm]	3,85	0.52
l_{22} [cm]	4,03	0,70
l_3 [cm]	3,50	0.10
l_4 [cm]	1,16	4.97
Creepage distance [cm]	55	47
creepage length reduction (%)	14.5	
Electric field at the pin region [kV/cm]	5,08	4.70
Electric field reduction at the pin region (%)	7.5	
Electric field at the cap region [kV/cm]	3.25	2.95
Electric field reduction at the cap region (%)	9.23	

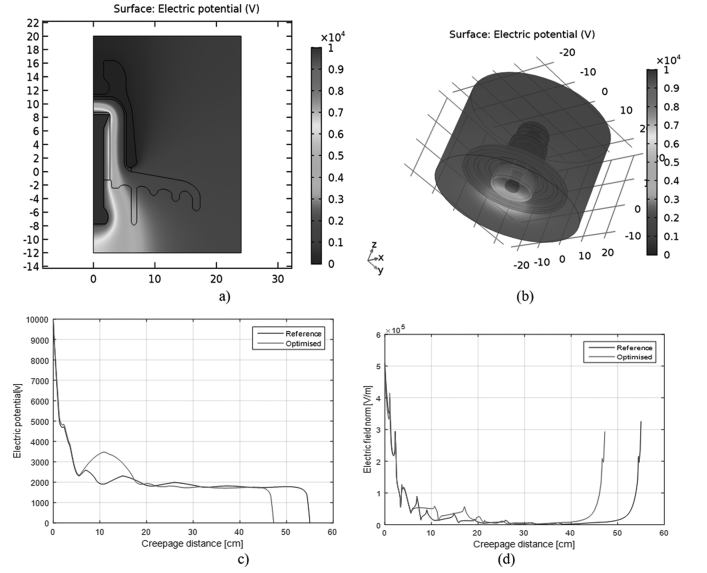


Figure 7. Clean case results after optimization. (a) 2D electric potential surface distribution; (b) 3D potential surface distribution; (c) potential distribution on the leakage path; and (d) electric field distribution on the leakage path.

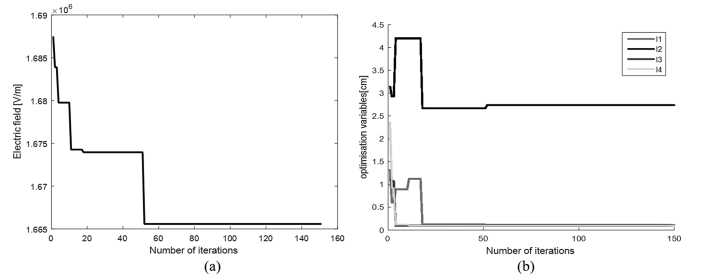


Figure 8. Optimization results in the polluted case. (a) The convergence curve and (b) the variation of the optimization variables.

is given in 2D and 3D representation in Fig. 7(a) and (b), respectively.

The distributions of the electric potential and the electric field on the upper surface of the insulator are given in Fig. 7(c) and (d), respectively.

2.4.2 Polluted Case

The same optimization procedure is done in the polluted case. After the optimization process, the convergence curve of the electric field along the iterations is given in Fig. 8(a), and the variation of the optimization variables are given in Fig. 8(b). The obtained shape of the insulator is shown in Fig. 9.

The details values of the optimized model are summarized in Table 4. Potential and electric field distributions are given in Fig. 10(a) and (b), respectively, in 2D and 3D representation.

The distributions of the potential and the electric field on the leakage path of the insulator are given in Fig. 10(c) and (d), respectively.

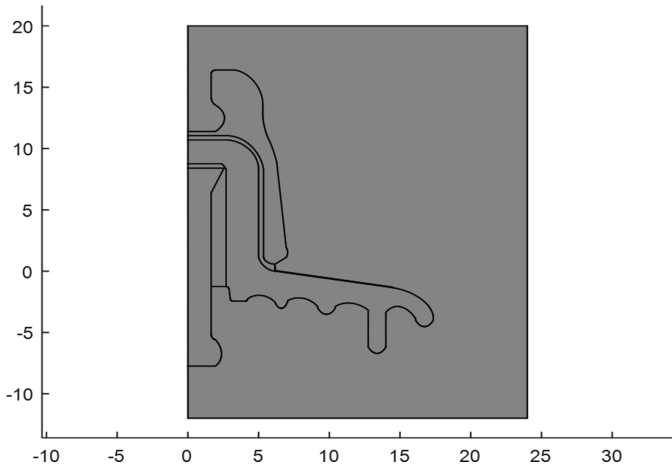


Figure 9. The shape of the obtained insulator after optimization (polluted case).

Table 4
Details of the Optimized Values in the Polluted Case

	Reference Model	Optimized Model
l_1 [cm]	3,30	0.11
l_{11} [cm]	3,40	0.21
l_2 [cm]	3,85	2.74
l_{22} [cm]	4,03	2.92
l_3 [cm]	3,50	0.10
l_4 [cm]	1,16	0.10
Creepage distance [cm]	55	39.22
Creepage length reduction (%)	28.7	
Electric field at the pin region [kV/cm]	17	16.66
Electric field reduction at the pin region (%)	2	

Although a little diminution of the electric field in the pin region, we notice an important decrease in the creepage distance.

3. Discussion

The results obtained in the polluted case before optimization show that the contamination has a significant effect on the electric field shape. This effect can be quantified as an important increase in the maximum value of the electric field near the pin and a decrease in the cap region [5].

The simulation results obtained after optimization in both clean and polluted cases show a significant decrease in the electric field values particularly near cap end.

It is clear that the proposed optimization approach has significantly reduced the maximum electric field near the pin end. For the polluted case also, a big similarity

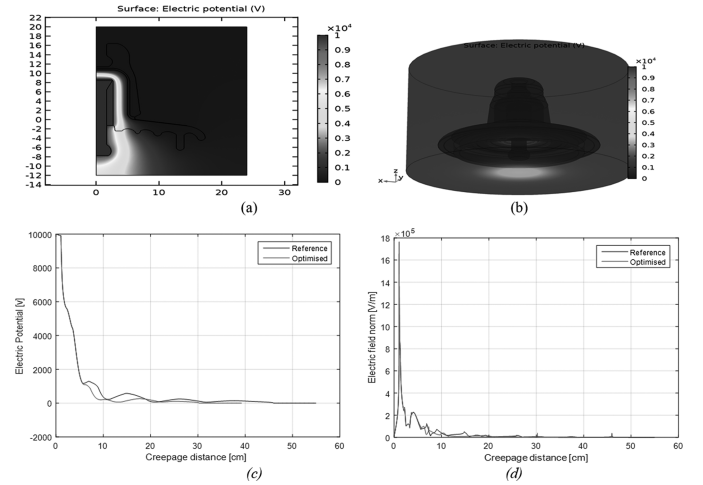


Figure 10. Polluted case results after optimization. (a) 2D electric potential surface distribution; (b) 3D potential surface distribution; (c) potential distribution on the leakage path (from the pin to the cap); and (d) electric field distribution on the leakage path (from the pin to the cap).

is observed with [11] and [12] using a predicted objective function with ANN.

4. Conclusion

An approach for optimizing HV suspension insulator under polluted conditions is proposed in this paper. FEM simulation was used to analyse the potential and the electric field distributions in 2D and 3D along the leakage path of U400B cap and pin insulator for both clean and polluted conditions. The proposed PSO approach searches the optimal variables (geometry) which minimize an objective function that is the electric field at the pin region. The most important achievements of this paper are summarized in the following points:

- In the clean case, the optimized model indicates a decrease of the electric field in the pin region with 7.5%, with a very significant decrease of the creepage distance around 14%. Adding to that, there is a drop in the electric field value at the cap region with 9.23%.
- In the polluted case, although we have no significant decrease in the electric field value at the pin region, the obtained shape gives a very reduced creepage distance (−29%) for approximately the same electric behaviour as the reference model.

References

- [1] D. Nie, H. Zhang, Z. Chen, *et al.*, Optimization design of grading ring and electrical field analysis of 800 kV UHVDC Wall bushing, *IEEE Transactions on Dielectrics and Electrical Insulation*, 20(4), 2013, 1361–1368.
- [2] K. Bhattacharya, S. Chakravorti, and P. K. Mukherjee, Insulator contour optimization by a neural network, *IEEE Transactions on Dielectrics and Electrical Insulation*, 8, 2001, 157–161.
- [3] W. S. Chen, H. T. Yang, H-Y. Huang, Optimal design of support insulators using hashing integrated genetic algorithm and optimized charge simulation method, *IEEE Transactions on Dielectrics and Electrical Insulation*, 15(2), 2008, 426–434.

- [4] W. S. Chen, H. T. Yang, and H. Y. Huang, Contour optimization of suspension insulators using dynamically adjustable genetic algorithms, *IEEE Transactions on Power Delivery*, 25(3), 2010, 1220–1228.
- [5] D. Doufene, S. Bouazabia, and A. Haddad, Optimized performance of cap and pin insulator under wet pollution conditions using a mono-objective genetic algorithms, *Australian Journal of Electrical and Electronics Engineering*, 16(3), 149–162. <https://doi.org/10.1080/1448837X.2019.1627740>.
- [6] S. Banerjee, A. Lahiri, and K. Bhattacharya, Optimization of support insulators used in HV systems using support vector machine, *IEEE Transactions on Dielectrics and Electrical Insulation*, 14, 2007, 360–367.
- [7] B. M’hamdi, M. Tegar, and A. Mekhaldi, Optimal design of corona ring on HV composite insulator using PSO approach with dynamic population size, *IEEE Transactions on Dielectrics and Electrical Insulation*, 23(2), 2016, 1048–1057.
- [8] D. Nie, H. Zhang, Z. Chen, *et al.*, Optimization design of grading ring and electrical field analysis of 800 kV UHVDC Wall bushing, *Transactions on Dielectrics and Electrical Insulation*, 20(4), 2013, 1361–1368.
- [9] D. Doufene, S. Benharat, S. Bouazabia, and S. A. Bessedik, Hybrid Grey Wolf and Finite Element Method (GWO-FEM) algorithm for enhancing high voltage insulator string performance in wet pollution conditions, *Engineering, Technology & Applied Science Research*, 12(3), 2022, 8765–8771.
- [10] D. Doufene, S. Bouazabia, and A. Haddad, Shape and electric performance improvement of an insulator string using particles swarm algorithm, *IET Science, Measurement & Technology*, 14(2), 2020, 198–205. <https://doi.org/10.1049/iet-smt.2019.0405>.
- [11] S. F. Stefenon, C. S. Furtado Neto, T. S. Coelho, *et al.*, Particle swarm optimization for design of insulators of distribution power system based on finite element method, *Electrical Engineering*, 104, 2021, 615–622. <https://doi.org/10.1007/s00202-021-01332-3>
- [12] D. Doufene, S. Bouazabia, and A. Haddad, Polluted insulator optimization using neural network combined with genetic algorithm, *18th International Symposium on Electromagnetic Fields in Mechatronics, Electrical and Electronic Engineering (ISEF)*, Poland, 2017.
- [13] D. Doufene, S. Bouazabia, and A. A. Ladjici, Shape optimization of a cap and pin insulator in pollution condition using particle swarm and neural network, *The 5th International Conference on Electrical Engineering – Boumerdes (ICEE-B)*, Boumerdes, Algeria, 2017.
- [14] S. Mirjalili, S. M. Mirjalili, and L. Andrew, Grey Wolf optimizer, *Advances in Engineering Software*, 69, 2014, 46–61.
- [15] E. Akbari, M. Mirzaie, M. B. Asadpoor, *et al.*, Effects of disc insulator type and corona ring on electric field and voltage distribution over 230-kV insulator string by numerical method, *Iranian Journal of Electrical and Electronic Engineering*, 9, 2013, 58–66.
- [16] A. J. Phillips, J. Kuffel, *et al.*, Electric fields on AC composite transmission line insulators, *IEEE Transactions on Power Delivery*, 23(2), 2008, 823–830.
- [17] V. T. Kontargyri, I. F. Gonos, *et al.*, Measurement and simulation of the electric field of high voltage suspension insulators, *European Transactions on Electrical Power*, 19, 2009, 509–517.
- [18] Y. Qing, S. Wenxia, D. Jiazhao, *et al.*, New optimization method on electric field distribution of composite insulator, *Annual Report Conference on Electrical Insulation and Dielectric Phenomena*, West Lafayette, IN, 2010, <https://doi.org/10.1109/CEIDP.2010.5724046>.
- [19] T. Doshi, R. S. Gorur, and J. Hunt, Electric field computation of composite line insulators up to 1200 kV AC, *IEEE Transactions on Dielectrics and Electrical Insulation*, 18(3), 2011, 861–867.
- [20] D. Doufene, S. Bouazabia, and R. Bouhaddiche, Heating dissipation study of a pollution layer on a cap and pin insulator, *2018 International Conference on Communications and Electrical Engineering (ICCEE)*, El Oued, Algeria, 2018, 1–4, <https://doi.org/10.1109/CCEE.2018.8634549>.
- [21] Y. Zhang, L. Li, *et al.*, Flashover performance test with lightning impulse and simulation analysis of different insulators in a 110 kV double-circuit transmission tower, *Energies*, 11, 2018, 659.
- [22] Global insulator Groupe, *Isolateurs pour lignes de transmission et stations de distribution à tension de 0,4 à 1150 KV*, Catalogue des produits, 2012.
- [23] R. Cook, *et al.*, *Concepts and applications of finite element analysis*, John Wiley & Sons, 1989.
- [24] R. Eberhart and J. Kennedy, A new optimizer using particle swarm theory, *Sixth Int’l. Sympos. Micro Machine and Human Science*, Nagoya, Japan, 1995, 39–43.
- [25] D. P. Rini, S. M. Shamsuddin, S. S. Yuhaniz, Particle swarm optimization: Technique, system and challenges, *International Journal of Computer Applications*, 14(1), 2011, 19–27.

Biographies



Dyhia Doufene graduated in 2008 from the University of Science and Technology Houari Boumediène (USTHB), Algeria, with a degree of “Ingénieur d’Etat” and then obtained the “Magister” degree from USTHB, in 2010. She received her Ph. D. degree in 2018 from the USTHB. Her research areas are mainly on high-voltage technology, outdoor insulation, optimization problems, and artificial intelligence.



Slimane Bouazabia was born in 1964 in Algeria. He received his Ph. D. degree in 2006 in Polytechnic School of Algiers. His interest domains are high-voltage technology, electrical discharges, and electric field calculation. Since 1988, he has assumed the role of professor (teaching and research) at Algiers University USTHB.



Sid A. Bessedik received the Ing. degree in electrical engineering from the University Ibn-Khaldun Tiaret, Algeria, in 2004 and Dipl. Magister in High Voltage from the University of Sciences and Technology of Oran (USTO), Algeria, in 2008. Since 2010, he joined the University Amar Telidji Laghouat, Algeria, as assistant professor and researcher at the LACoSER laboratory. His main research interests include high-voltage insulation, electromagnetic interference, fault diagnosis of induction motors, optimization, and artificial intelligence methods.